

DESIGN AND CONSTRUCTION OF A SCANNING TUNNELING MICROSCOPE
FOR ATOMIC SCALE IMAGING OF SURFACES IN ULTRA-HIGH VACUUM

THESIS

Presented to the Graduate Council of
Texas State University-San Marcos
in Partial Fulfillment
of the Requirements

for the Degree

Master of SCIENCE

by

Robert S. Kilbourn, B.S.

San Marcos, Texas
May 2010

DESIGN AND CONSTRUCTION OF A SCANNING TUNNELING MICROSCOPE
FOR ATOMIC SCALE IMAGING OF SURFACES IN ULTRA-HIGH VACUUM

Committee Members Approved:

Carl A. Ventrice, Jr., Chair

Heather C. Galloway

Wilhelmus J. Geerts

Approved:

J. Michael Willoughby
Dean of the Graduate College

COPYRIGHT

by

Robert S. Kilbourn

2010

ACKNOWLEDGEMENTS

Thank you to my father and stepmother for always believing in me and giving me the support that I needed to succeed to this point. Graduate studies have been very enlightening and I am proud that I could follow in your footsteps and go further in the pursuit of knowledge. I would also like to thank my brother David for always pushing me to be dedicated and to always believe in myself even when others don't and times are dark.

Most of all I would like to thank Carl for your unwavering patience and countless hours you have spent working with me on this project. Your dedication to teaching and research is truly an inspiration to me and something that I look up to immensely, I could not have completed this project without your mentorship.

Thanks to my classmates Jen, Chris, Nick, Simona. I would never have gotten through the coursework if it were not for you guys being there with me, everyone coming together and pushing each other to be the best at physics no matter what the situation.

Finally, thank you to my friends for always being there for me especially my band mates Mike, Collin and Xavier music helped me deal with the stresses of grad school. I would also like to give a special thanks to my friends Mike and Laura for your understanding and standing up for me you two are incredible friends.

This manuscript was submitted on December 16th 2009.

.

TABLE OF CONTENTS

	Page
ACKNOWLEDGEMENTS	iv
LIST OF FIGURES	vi
ABSTRACT	viii
 CHAPTER	
I. INTRODUCTION	1
II. THEORY OF SCANNING TUNNELING MICROSCOPY	3
III. DESIGN AND OPERATION OF INSTRUMENT	16
A. Ultra High Vacuum	16
B. Vibration isolation and operational stages	22
C. Thermal isolation	29
D. Design of Macor STM assembly	31
E. Machining Methods	35
F. Electronics Design	41
IV. RESULTS AND DISCUSSION	44
V. CONCLUSIONS	50
REFERENCES	51

LIST OF FIGURES

Figure	Page
1. Quantum mechanical tunneling of an electron through a rectangular potential barrier	4
2. Inchworm motor operations	8
3. Tube scanner operation	9
4. Motion of a tip scanner	10
5. Constant current scanning mode	14
6. Ultra-high vacuum pump system	20
7. STM assembly inside the chamber in the locked position drawn to scale 1:5	23
8. Three operating positions of the STM, scale 1:3	28
9. Sample holder assembly parts drawn 1:1 scale with a hole size table for the Macor sample mounting plate	33
10. A 1:1 scale drawing of the STM head assembled with the Burleigh ARIS-11 approach module mounted	34
11. Geometry of standard threads	37
12. STM control electronics	43
13. UHV surface analysis chamber	44
14. STM components	45
15. STM mounted on test stand	46
16. STM head with tip and UHV inchworm	47

17. STM sample mount and electrical connections	47
18. STM in locked, floating, and raised position	48

ABSTRACT

DESIGN AND CONSTRUCTION OF A SCANNING TUNNELING MICROSCOPE FOR ATOMIC SCALE IMAGING OF SURFACES IN ULTRA-HIGH VACUUM

by

Robert S. Kilbourn, B.S.

Texas State University-San Marcos

May 2010

SUPERVISING PROFESSOR: CARL A. VENTRICE JR.

The goal of this research project was to design and build a scanning tunneling microscope to be used in the ultra-high vacuum based surface analysis system in the Surface Science Laboratory at Texas State University-San Marcos. The instrument that was constructed is designed to produce atomic-scale images on single crystal samples and to allow transfer of samples to the horizontal manipulator of the system for surface preparation and high-resolution electron energy loss spectroscopy measurements. The outer layer of atoms of most materials either relax or reconstruct, which often results in a change in the electronic, magnetic, and/or chemical properties. Therefore, it is important to be able to

characterize the geometric structure of the surface of a material if one is to understand the effect of surface interactions. The main body of the scanning tunneling microscope is constructed from Macor, which is a machinable ceramic. Macor is ultra-high vacuum compatible and has a high strength to weight ratio, low thermal expansion coefficient, and low thermal conductivity, which are all properties desirable for atomic scale imaging. The instrument is mounted on springs with a 13'' extension length, which gives it a resonant frequency of less than 1 Hz for vibration isolation. The tube scanner is mounted to an ultra-high vacuum compatible inchworm for coarse and fine approach of the tip to the sample surface. Custom designed analog electronics and software are used to control the instrument.

I. INTRODUCTION

Scanning tunneling microscopy (STM) is an experimental technique that is capable of measuring the atomic scale features of surfaces. Most STM studies are performed in ultra-high vacuum (UHV) since the surfaces of most materials will oxidize or be contaminated under ambient conditions. The goal of this research project was to build a UHV STM for atomic scale analysis of surfaces at room temperature. The instrument was designed so that it could be incorporated into an existing UHV analysis chamber in the Surface Science Laboratory at Texas State. This chamber has standard sample preparation techniques including an ion gun for cleaning surfaces, an electron beam evaporator for depositing metal films, low energy electron diffraction (LEED) optics, and a high resolution electron energy loss spectroscopy (HREELS) spectrometer. Therefore, the design of the STM allows transfer of samples between the *xyz* manipulator of the system and the STM and also has sufficient internal vibration isolation to allow atomic resolution imaging.

This project focused on the design, construction, and assembly of the mechanical components of the STM. The initial stages of the STM project included the design of the STM electronics and the software to control the STM. These tasks were performed by Prof. Ventrice's research group when he was a professor at the University of New

Orleans. The mechanical design of our STM is based on a previous STM that was constructed at Rensselaer Polytechnic Institute (RPI) for imaging the surfaces of 2" wafers within a molecular beam epitaxy (MBE) system [1]. The UHV vacuum system in the Surface Science Lab is primarily designed for surface science studies of both single crystal metals and semiconducting materials that are no larger than ½" x ½" in size. Therefore, the sample mounting and transfer mechanism needed to be redesigned. At the time that this project was started, the inchworm motor, which is used for the coarse and fine approach of the STM tip, and its controller were already acquired. The first stage of the project was to design the mechanical components of the STM. The second stage was the machining of all of the individual components of the STM. This was followed by cleaning of the parts and assembly of the STM itself. In order to test the mechanical design of the STM, a platform was constructed since the UHV chamber was being used for measurements of the growth of graphene on Pt(111) by another graduate student (Greg Hodges) in our research group.

II. THEORY OF SCANNING TUNNELING MICROSCOPY

The scanning tunneling microscope (STM) uses quantum mechanical tunneling to image surfaces at the atomic level. Electrons tunnel from a sharp metallic tip, across a vacuum barrier, and into the sample that is imaged or in the opposite direction, depending on the polarity of the tip voltage. The characteristics of quantum mechanical tunneling are illustrated using a simple one-dimensional rectangular barrier, as shown in Figure 1. A current of electrons is incident on a potential barrier of height U_0 and spatial width L . Classically, when the electrons have energy less than the barrier height, there is zero probability that the electrons will penetrate the barrier since this would correspond to a region with negative kinetic energy. However, when the wavelike nature of the electron is considered, there is a small probability that the electrons will transmit through the barrier. [2]

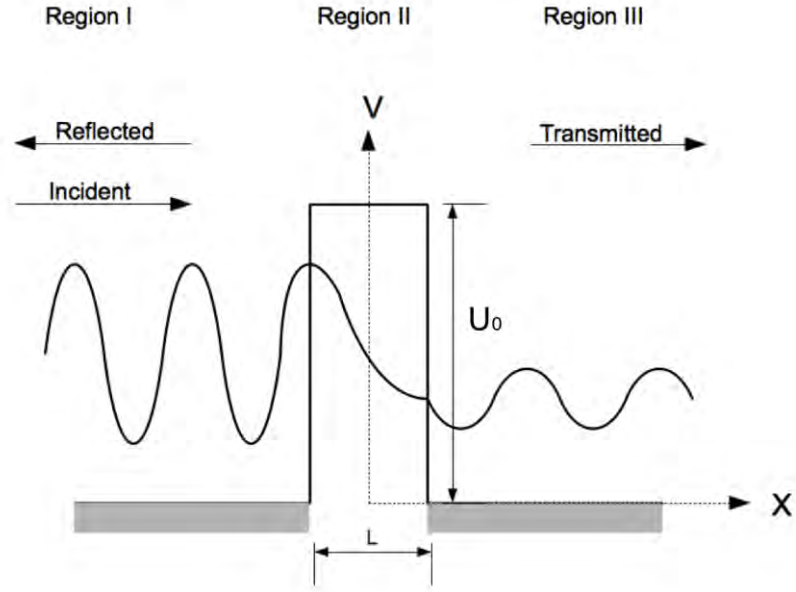


Figure 1: Quantum mechanical tunneling of an electron through a rectangular potential barrier

The wave functions of the electrons are found by solving the time independent Schrödinger equation in the regions I, II, and III, with potentials $U_I = 0$, $U_{II} = U_0$, and $U_{III} = 0$, respectively. This results in the following wave functions:

$$\psi = Ae^{ikx} + Be^{-ikx} \text{ (region I)} \quad (1)$$

$$\psi = Ce^{\alpha x} + De^{-\alpha x} \text{ (region II)} \quad (2)$$

$$\psi = Ge^{ikx} \text{ (region III),} \quad (3)$$

where the wave vector k and the constant α are given by

$$k = \frac{\sqrt{2mE}}{\hbar} \quad (4)$$

$$\alpha = \frac{\sqrt{2m(U_0 - E)}}{\hbar}. \quad (5)$$

To solve for the coefficients B , C , D , and G in terms of A , the wave function and its derivative with respect to x must be continuous at both boundaries of the barrier. The probability current in each region is given by [3]

$$j(x,t) = \frac{i\hbar}{2m} \left(\psi \frac{\partial \psi^*}{\partial x} - \psi^* \frac{\partial \psi}{\partial x} \right). \quad (6)$$

The transmission probability is found by taking the ratio of the probability current in region III to the probability current in region I and is given by

$$T = \frac{j_t}{j_i} = \left(\frac{1 + (k^2 + \alpha^2)}{(4k^2\alpha^2)\sinh^2(\alpha L)} \right)^{-1} \quad (7)$$

where j_t is the transmitted current density and j_i is the incident current density. When E is much less than the barrier height, equation 7 can be simplified by using the definition of $\sinh(x)$,

$$\sinh(x) = \frac{e^x - e^{-x}}{2}, \quad (8)$$

resulting in the following expression for the transmission coefficient

$$T = \frac{j_t}{j_i} = \left(1 + \frac{(k^2 + \alpha^2)}{(4k^2\alpha^2)} \left(\frac{e^{2\alpha L} - e^{-2\alpha L}}{4} \right) \right)^{-1}. \quad (9)$$

When αL is greater than 1, the decaying exponential term can be neglected. For example If αL is equal to 1 then the decaying exponential term is 98% less than the increasing term. This results in the following expression for the tunneling probability

$$T \approx \frac{16k^2\alpha^2}{(k^2 + \alpha^2)^2} e^{-2\alpha L}. \quad (10)$$

This approximation shows that there is an exponential dependence of the transmitted current density on the tunneling distance L . [4] When the width of the barrier is changed by a small amount, the current will change by an exponential factor. For a 5 eV barrier, a kinetic energy of 1 eV, and a barrier width of 1 Å, the transmission factor will change by a factor of ten when the potential barrier width changes by 1.2 Å.

The actual tunneling geometry of the STM tip is more complicated than a standard square barrier. For instance the work function of the tip and sample are usually different, and the sample is biased with respect to the tip. Therefore, the actual tunneling geometry is more accurately modeled as a trapezoidal potential barrier. This more complicated geometry can be solved by other methods including the transfer Hamiltonian approach and semi-classical perturbation treatment (*WKB*). The transfer Hamiltonian

method uses an arbitrary potential to solve this problem. [4] The WKB method uses a first order series approximation. [5] In both cases the transmission current density shows an exponential dependence on the barrier width.

To make a reliable measurement of tunneling current, a preamp that can accurately measure currents of 10^{-9} A is needed. In addition, the STM must be able to maintain the distance between tip and sample, which is typically ~ 1 Å, with an accuracy of about 0.1 Å or better. This precise positioning of the tip-sample distance is achieved by using piezoelectric materials. Piezoelectric materials are used in STM because they can distort their shape in very small and predictable amounts when an electric potential is applied. This distortion depends on the type of piezoelectric material, its geometry, and the location and strength of the applied potential.

The tip will need to approach the sample from a distance many orders of magnitude larger than the distance needed to maintain stable tunneling. The tip will also need a mechanical method to scan across the surface of the sample to reveal the atomic scale features of the surface. These requirements are met by using a two-step system, with a mechanism for course approach and a mechanism for maintaining a stable tunneling current and for scanning the surface. Both of these systems use piezoelectric drives.

The course approach mechanism that our STM uses is an inchworm motor manufactured by Burleigh Instruments, Inc. This type of motor uses two piezo clamps and a piezo spacer that expands and contracts to move the tip in a linear fashion. A schematic of the operation of an inchworm motor is shown in Figure 2.

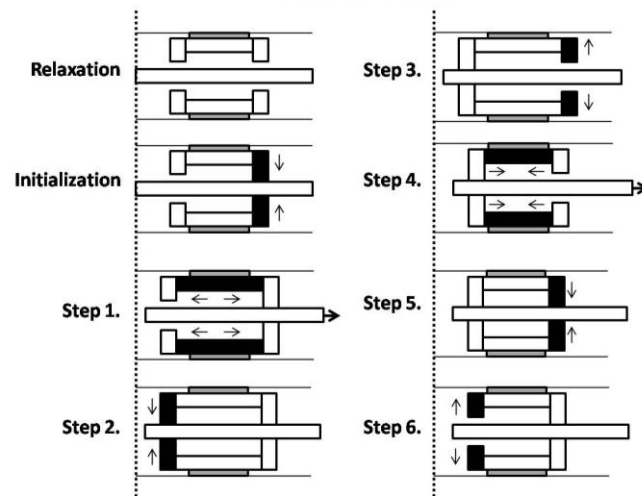


Figure 2: Inchworm motor operations

An inchworm controller is used to apply the voltages in the correct order to the inchworm motor. The controller receives several TTL signals from the DAC of the control computer. One TTL signal tells the controller the direction of the motion of the inchworm, another TTL is used to start and stop the motion of the inchworm, and a high frequency series of TTL pulses is used to control the speed of the inchworm. [6] The inchworm controller also has a disconnect feature that isolates the inchworm piezos after stable tunneling is achieved, which prevents motion of the inchworm from electrical noise and ripple on the high voltage drivers. This signal from the computer is at a relatively high frequency, so a shielded cable is used to prevent coupling to the signals that drive the inchworm motor.

A tube scanner is used for the control of the sample-tip distance and the X and Y scanning motion across the sample. A tube scanner consists of a piezo tube with an electrode mounted on the inside of the tube so that applied potentials will expand or contract the tube for z-axis movement. Movement in the x and y directions is achieved by having four electrodes mounted ninety degrees apart on the long axis of the outside of the tube as shown in Figure 3.

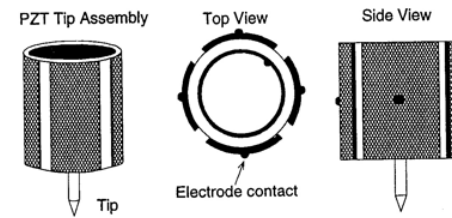


Figure 3.6. A PZT ceramic made into a hollow cylinder

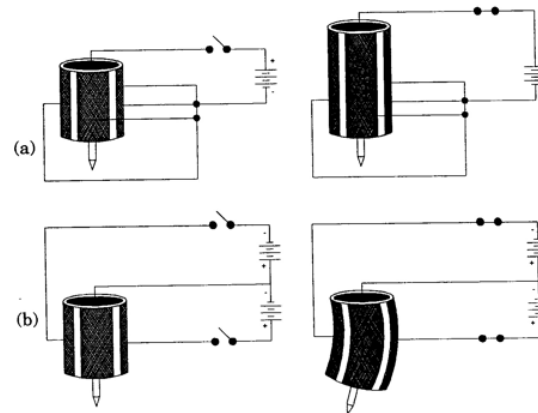


Figure 3: Tube scanner operation taken from ARIS-10/11 approach module operating manual. [6]

The X or Y scanning is achieved by applying a differential voltage ($\pm V_x$ or $\pm V_y$) on opposite quadrants of the tube while maintaining a constant potential of V_z on the inside

of the tube scanner. This results in a bending of the tube in either the x or y direction, depending on which quadrants are biased. The bending motion leads to small changes in the z -direction because of the arc like movement of the tip that is mounted on one end of the center of the tube as shown in Figure 4.

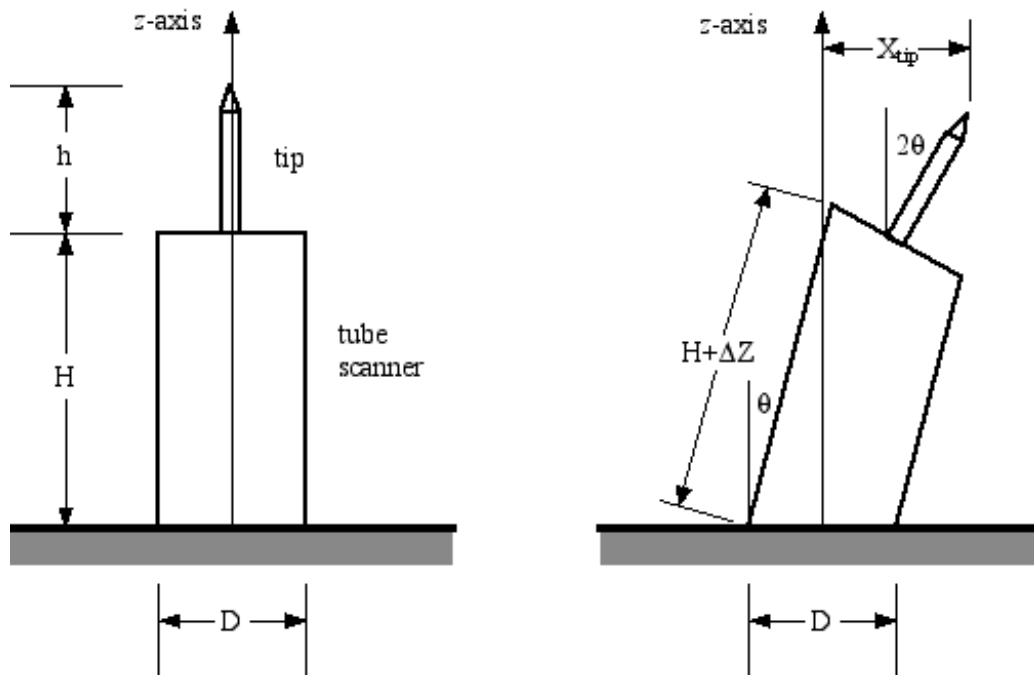


Figure 4: Motion of a tip scanner

These z -axis movements will result in an output from the feedback control system to maintain a constant tunneling current, which will distort the image. The amount the tip displaces in the z -direction can easily be predicted, and the imaging software can be used to compensate for this effect. The tip movement in each direction (x , y , and z) can be derived from trigonometric relationships. When a differential voltage is applied across

opposite quadrants, one side of the tube will contract by an amount ΔZ and the other will expand by that same amount. From figure 4 it can be shown that

$$\tan\theta = \frac{\Delta Z}{D}. \quad (11)$$

The contraction and expansion of the piezoelectric is small, therefore the small angle approximation,

$$\begin{aligned} \sin\theta &\approx \theta \\ \cos\theta &\approx 1 - \frac{\theta^2}{2} \end{aligned} \quad (12)$$

is used. Since

$$\tan\theta = \frac{\sin\theta}{\cos\theta}, \quad (13)$$

equation 11 becomes,

$$\theta \approx \frac{\Delta Z}{D}. \quad (14)$$

The displacement in the x -direction of the top of the scanning tube is found by,

$$X_{top} = H \sin \theta \approx H \theta = \frac{\Delta Z}{D} H. \quad (14)$$

The displacement in the z -direction becomes,

$$Z_{top} = H \cos \theta \approx H \left(1 - \frac{\theta^2}{2}\right) = H \left[1 - \frac{\Delta Z^2}{2D^2}\right]. \quad (15)$$

The imaging corresponds to the motion of the apex of the tip. For a tube scanner tilt angle θ , the tip tilt angle is 2θ . The amount that the apex of the tip moves in the $x(y)$ and z -directions is given by equations 16 and 17,

$$X_{tip} = X_{top} + h \sin 2\theta = \frac{\Delta Z}{D} (H + 2h) \quad (16)$$

$$Z_{tip} = Z_{top} + h \cos 2\theta = H + h - \frac{\Delta Z^2}{2D^2} (H + 4h). \quad (17)$$

The change in height of one side of the tube (ΔZ) can be found by using the piezoelectric gain of the material, which is a measurement of how much the length changes due to an applied potential. The Z -gain of the piezoelectric tube scanner used for our STM is approximately $G_z = \Delta Z/V_z = 35 \text{ \AA/V}$. Therefore, the tip displacement in the $x(y)$ -directions for a tube scanner that is $H = 0.5''$ high and $D = 0.25''$ wide and tip that is $h = 0.25''$ high with a $\pm 1\text{V}$ differential bias is $\Delta X(\Delta Y) \approx 140 \text{ \AA}$. In other words, $G_x = G_y = 140 \text{ \AA/V}$. For this same differential bias, the z -axis shortens by $Z_{bow} = Z_{tip} - (H + h) = 6 \times$

10^{-5} Å. However, if a ± 100 V differential bias is applied, the displacements become $\Delta X(\Delta Y) \approx 1.4 \mu\text{m}$ and $Z_{bow} = 2.3$ Å

Once there is a reliable method of tip approach and scanning, the process of measuring the current and creating an image must be considered. There are two common modes of operation of an STM: constant height imaging (CHI) and constant current imaging (CCI). CHI is where the tip is kept at a constant height above the sample and the current is measured as the tip is scanned across the sample. This is a less common used mode of operation because of two major limitations. The surface needs to be relatively smooth so that the tip does not come in contact with the sample. The barrier height would also need to be known as a function of location to learn any specific spatial information about the surface. CCI is the most widely used STM imaging mode. CCI uses a feedback loop to drive the z -axis so that the tip is kept at a constant current determined by a reference current shown in Figure 5. [4]

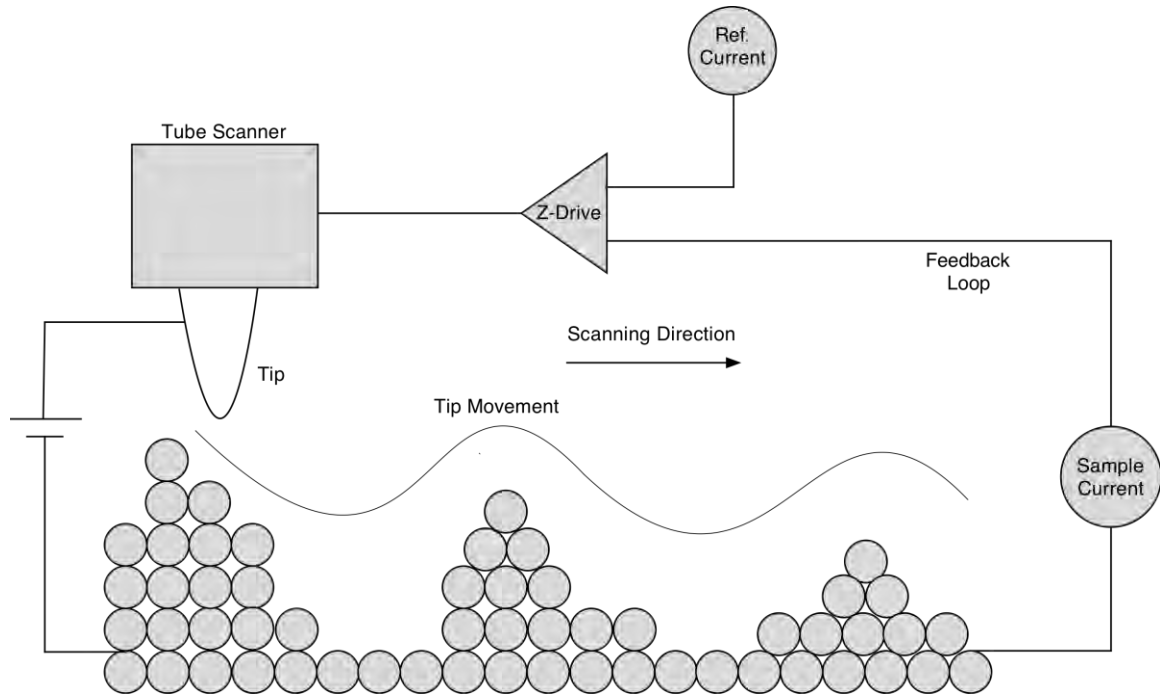


Figure 5: Constant current scanning mode

The speed of scanning is limited in CCI due to the response time of the feedback loop and the resonant frequency of the STM scanning head [4]. This can affect the spatial resolution if the surface features are closely spaced. When designing the electronics for the feedback loop, high frequency response and low noise are required.

The features imaged in the CCI mode correspond to a spatial map of constant tunneling probability, which does not necessarily correspond to the positions of the atoms at the surface. The STM is probing occupied or unoccupied states of the surface atoms on the sample. The tip bias determines the electronic state being probed. This means that there can be states that will extend into the vacuum barrier or into the bulk depending on the material used for the tip and the sample [4]. To get spatial information from the

images, the density of states (DOS) information must be analyzed as a function of position, which is accomplished by performing scanning tunneling spectroscopy (STS) as described below. In CCI mode spatial information can be obtained easily from the voltage output of the feedback loop that controls the height of the tip since Z is proportional to V_z . This direct spatial information along with the DOS measurements from the tunneling current can be used to determine the atomic structure of surfaces.

As mentioned above, spectroscopic measurements can also be taken with an STM. If the tip is held at a constant z position and the sample bias is changed, I-V curves can be produced. If CCI is being used, the feedback loop must be disabled while the sample bias is modulated. These measurements are done over a range of positions and a range of different tip bias values. These values can be compared to obtain electronic DOS of the sample. Semiconductor properties can be measured when using this mode of probing including accurate band gap measurements. [7]

Mechanical vibrations and thermal drift can affect the measurements significantly. The design must minimize all sources of vibration over a large frequency range. Materials that have low thermal expansion should be chosen for the tip and sample holder to prevent the tip from changing position due to local changes in the temperature of the instrument. These are the largest sources of error in any STM mode and will significantly reduce the resolution if not addressed. The sample and the tip need to be as clean as possible, which is achieved by performing tunneling inside an ultra high vacuum (UHV) environment.

III. DESIGN AND OPERATION OF INSTRUMENT

A. Ultra High Vacuum

UHV is an environment with pressures on the order of 10^{-11} Torr; this value is about 13 orders of magnitude lower than atmospheric pressure. Under these conditions particles in the chamber have a mean free path of distances that are at least as large as the chamber dimensions. This calculation comes from the derivation of the mean free path using a kinetic theory approach that incorporates the average relative velocity because of the random movement of all of the gas molecules. This is shown in equation 18

$$\lambda = \frac{RT}{\sqrt{2}\pi d^2 N_A P} \quad (18)$$

where R is the gas constant, T is the absolute temperature in Kelvin, N_A is Avogadro's number, P is pressure and d is the collision diameter of the molecule. [8] This relationship also implies that there is a relatively low number of molecules that collide with the sample surface every second when under UHV. The flux of molecules impinging on the surface is given by

$$\Phi = (3.513 \times 10^{22}) \frac{P}{\sqrt{MT}} \text{ molecules/cm}^2 \cdot \text{s}, \quad (19)$$

where M is the molecular weight and P is the pressure in Torr. [9] Inverting this equation and multiplying it by the density of surface atoms (D_a) given in molecules/cm² gives the time it takes to form a monolayer

$$t = \frac{D_a (MT)^{1/2}}{(3.53 \times 10^{22}) P} \quad (20)$$

for atmospheric pressure, this relationship gives a time of $\sim 10^{-9}$ seconds to form a monolayer at room temperature if it is assumed that the gas is composed primarily of N₂ and the molecules all dissociate. If a sample is under a vacuum of $\sim 10^{-10}$ torr, the time to form a monolayer increases to ~ 10 hours. This approximation assumes that every gas atom that hits the surface will stick and dissociate. Under most conditions, this is not the case. One can modify equation 20 to introduce a sticking coefficient S .

$$t = \frac{D_a (MT)^{1/2}}{(3.53 \times 10^{22}) PS} \quad (21)$$

This shows that UHV conditions are ideal for the use of STM, which requires a very clean sample surface.

The process to reach UHV is a multistage pumping process that uses different types of pumps to reach pressures in the range of 10^{-11} Torr. The first stage uses mechanical pumps that take the chamber from atmospheric pressure to around 10^{-3} Torr. The most common mechanical pumps use rotary vanes that spin inside a cavity to evacuate the gases from the chamber. These pumps use oil to lubricate and seal the internal mechanisms. Since the oil is exposed to vacuum, it will partially vaporize, and this oil vapor can backstream into the chamber during operation. To avoid this, a trap must be placed between the pump and the chamber.

The vacuum limit of a rotary vane pump is 10^{-3} Torr. Therefore, turbo molecular pumps are used to pump from 10^{-3} to 10^{-11} Torr. These pumps use multiple stacks of fans that are mounted on a spinning shaft. The rate of this rotation depends on the size of the turbo pump and can be as high as 80,000 RPM. The fans impart momentum on the gas molecules that diffuse into the intake of the pump sending them toward the exhaust side of the turbo where a mechanical pump is used to pump the gas out of the turbo. Most Turbomolecular pumps should only be operated at or below 10^{-3} Torr to prevent excess drag on the pump, which causes heat to build up in the pump's bearings. Therefore, bearings will fail easily if a turbo is run near atmospheric pressure. [9]

Another type of pump that works in parallel to the turbo is the ion pump. Ion pumps use an electric field to emit electrons that can then ionize gas molecules in the chamber, which are then accelerated into Ti plates that capture the gas molecules. These pumps use magnets to cause the field emitted electrons to spiral, resulting in an increased probability of ionizing a gas molecule. This pump uses no oil and does not have any mechanical parts, making it very reliable and clean. Ion pumps are not very effective in

pumping hydrogen atoms, so a different type of pump is used for this purpose. A titanium sublimation pump (TSP) is used to trap reactive gas molecules such as hydrogen. This type of pump works by evaporating a fresh layer of Ti onto the surface of the pump housing. This layer of titanium then reacts with the gas molecules inside the chamber. [9]

Valves are put on the intake side of each pump so they can be individually controlled during the pumping process. There is also a load lock that has a valve so that samples can be introduced to UHV without venting the entire chamber. The valve on the main turbo pump of the STM chamber is a pneumatically controlled gate valve. In case of a power failure, this valve will close to prevent the chamber from backfilling with air as the turbo pump winds down. This entire system is illustrated in Figure 6.

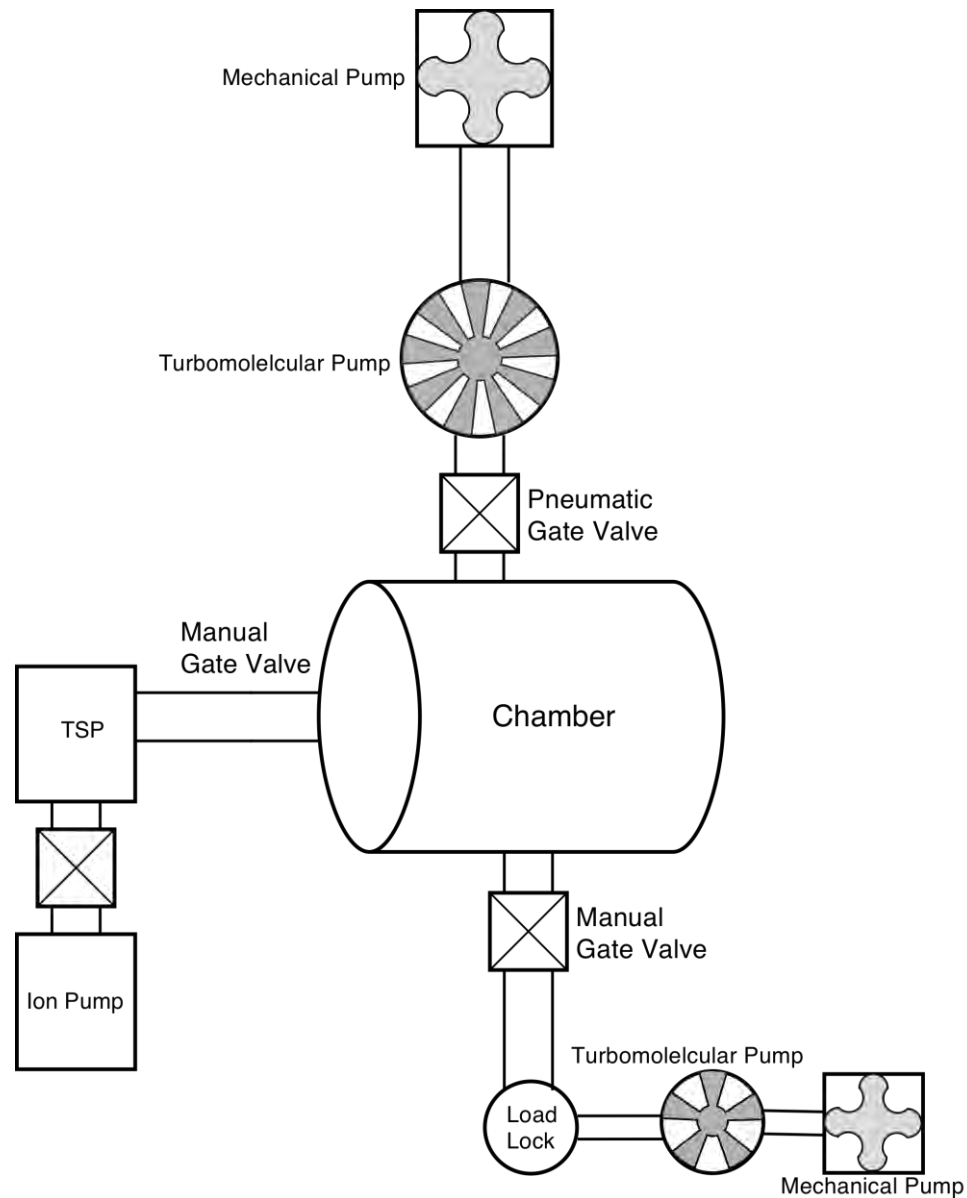


Figure 6: Ultra-high vacuum pump system

When the chamber is first pumped down after being exposed to atmospheric pressure, water and other molecules that adsorbed on the internal surfaces of the chamber will start to evaporate, limiting the ultimate vacuum achieved by the pumps in a reasonable pumping time. To desorb these molecules, the entire chamber is heated to a

temperature of about 150°C for at least 24 hours. Heat tapes are wrapped around the entire chamber and controlled by variable voltage power supplies (Variacs). The mechanical and electronic parts that will be under UHV must be carefully designed to handle the prolonged high temperatures of the bake out.

Materials that have low evaporation pressures under bake out temperatures are used. Wire insulation and adhesives are chosen to be compatible in UHV. The parts must be thoroughly cleaned to remove any oil or dirt residue from the manufacturing process. All blind screw holes must be vented by using a degas hole or by using a vented screw. The degas hole is drilled at the bottom of a hole typically perpendicular to the hole being vented. The most important issue is to make sure that the bottom of the hole has a way to vent the gas that gets trapped between the bottom of the screw and the bottom of the tapped hole. All of the surfaces should be machined very smooth to keep outgassing to a minimum.

The metals that are used under UHV must be resistant to corrosion or oxidation. Stainless steel (SS) is used for most of the mechanical parts including the chamber. The most common stainless steel used for vacuum components is SS304, which is a non-magnetic alloy of 18-20% Cr, 8-12% Ni, 2% Mn, and 0.75% Si, with the balance being Fe. [10] The addition of Cr and Ni results in a surface $\text{Cr}_2\text{O}_3/\text{NiO}$ overlayer that makes it resistant to corrosion.

B. Vibration isolation and operational stages

The main section of the STM chamber has a diameter of 14". The STM is suspended in an 8" diameter can that is 15" high and attaches to a 10" conflat flange on the topside of the STM chamber. Below the chamber is another 10" conflat flange that holds the STM support. A magnetic translator is used to move samples into the STM chamber from the load lock. A horizontal x,y,z manipulator is used to move the sample from the STM section of the chamber to the sample prep section. A wobble stick is used to move the sample from the STM to the x,y,z manipulator or the magnetic translator and is also used for exchanging tips. A push pull device is used to raise and lower the STM to allow transfer of samples from the load lock to the x,y,z manipulator and to permit tip changes and mounting of the sample on the STM. Figure 7 shows the STM inside the chamber.

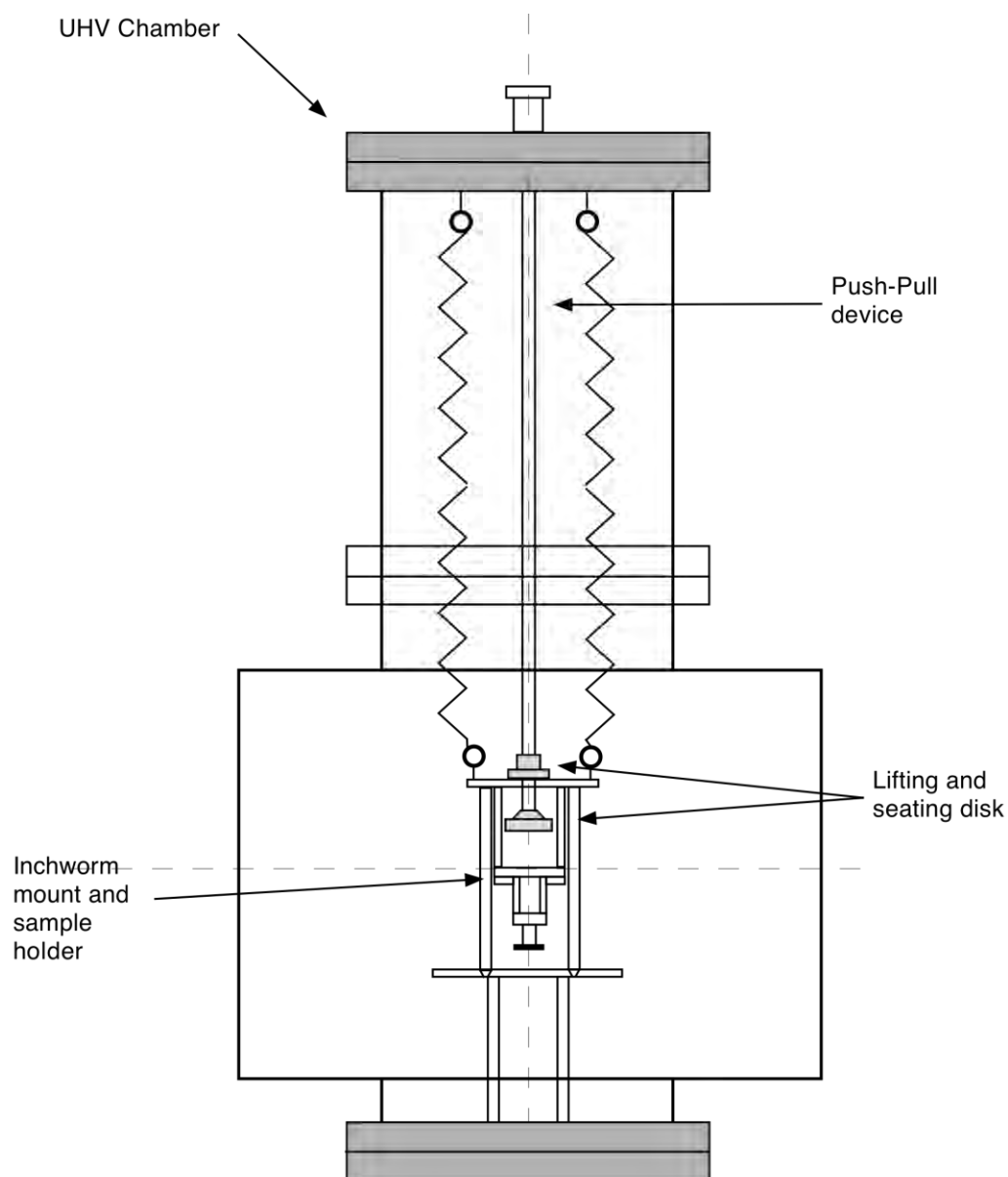


Figure 7: STM assembly inside the chamber in the locked position drawn to scale 1:5

Mechanical vibration isolation of the inchworm-sample holder assembly is very important since it allows us to achieve atomic resolution. The biggest sources of vibration are from the different pumps that transfer vibration to the walls of the chamber. The main turbo-molecular pump operates at a rotational speed of 45 kHz and the small

turbo that is connected to the load lock operates at 72 kHz. However, the rotary vane pumps, which operate with a rotational speed of 1800 Hz, couple more strongly to the STM head. Building sway and vibrations can also affect the performance of the STM. To prevent coupling to the building's motion, the STM chamber should be kept on the ground floor, if possible. In our case, the chamber is on the second floor, so internal vibration isolation of the STM head is very important. Since most of the sources of vibration are 1 kHz or higher, it is important that the resonant frequency of the vibration isolations system be as low as possible to decouple the STM from these sources of vibration. [1]

A spring suspension system with viton dampers is used to isolate the STM from the chamber. To find the resonant frequency of the STM head, which is supported by four parallel springs, the frequency dependence of a simple spring-mass system is analyzed. Hooke's Law describes the force exerted by a stretched spring,

$$F = -k(\delta x), \quad (22)$$

where δx is the amount the spring displaces from its free length and k is the spring constant in N/m. Using Newton's Second Law results in the following differential equation

$$\delta x'' + \frac{k}{m} \delta x = 0. \quad (23)$$

The constant k/m is defined as

$$\omega^2 = \frac{k}{m} . \quad (24)$$

This differential equation has solutions that have sinusoidal behavior

$$x(t) = A \cos(\omega t + \phi) . \quad [11] \quad (25)$$

When the spring-mass system is in equilibrium, the gravitational force (mg) is equal to the spring force

$$W = mg = kx_0 , \quad (26)$$

where x_0 is the distance the spring extends when the mass is at equilibrium. From Equations 25 and 26, it can be seen that the angular frequency only depends on g and x_0

$$\omega = \sqrt{\frac{g}{x_0}} . \quad (27)$$

Therefore, the resonant frequency of the system is

$$f = \frac{\omega}{2\pi} = \frac{1}{2\pi} \sqrt{\frac{g}{x_0}} \quad (28)$$

and only depends on the extension length x_0 of the spring if the mass of the STM head is constant. The extension length x_0 is chosen to be as large as possible to give the lowest resonance frequency. The distance from the top of the STM can to the center of the STM chamber is 24.5". However, the STM must float above the centerline during operation, and the length of the spring mounts, viton dampers, and the sample support assembly must also be subtracted from this distance. After taking these distances into account, the length of the springs plus their extension length was determined to be 16.4" when the STM is in the floating position. The spring stock that was chosen for use in the manufacture of the springs for the STM has a wire diameter of 0.015" with a 0.25" OD. The length of spring that was needed to give us the proper extension length was 3.1" from mounting loop to mounting loop. This gives an extension length of ~13.3" and a frequency of ~0.86 Hz. The frequency measured after construction of the instrument was ~1Hz. The design includes adjustable spring mounts that use an L bracket with a threaded rod 2" long that fit into threaded holes on the top plate so that the spring length can be fine-tuned. For instance, minor adjustments may need to be made after the STM has been exposed to bake out temperatures. The assembly floats in the chamber in a position where the sample holder is approximately 1" above the centerline of the chamber. The tip approach can be monitored using an optical microscope that looks through a window that is 45 degrees below the centerline of the chamber. The bottom plate was designed so that the line of sight to the tip from this window was not restricted.

The wiring is designed to limit vibration transfer to the STM head. We used Capton coated wire that is 0.005" in diameter for all connections between the electrical feedthrus on the STM mounting flange and the electrical terminals on the STM top plate.

The electrical terminals on the top plate are made from Mo pins glued into Macor mounts that attach to the sides of the top plate. Wire that has a diameter of 0.010" is used to connect the inchworm tube scanner and sample bias to the terminals on the top plate.

The entire instrument is designed to be very rigid so that vibrations are not easily transferred into the STM assembly. Counter boring the positions where the support rods are mounted to the sample mounting plate, top and bottom plates makes the assembly very stiff. Counter boring is where a round slot is machined 0.050" deep centered on the screw hole, the support rods fit inside these slots. Twisting and bending of the STM assembly will be limited with counter bored support mounts.

There are three operating positions of this STM, raised, locked and as described above the floating position. These different positions are controlled with a push pull device that is coupled to the instrument by two disks that are mounted to the center rod above and below the top plate. The center rod has a smaller diameter than the center hole in the top plate so that the push pull device is isolated from the STM assembly when in the floating position. The upper disk pushes the STM assembly into four tapered holes in the bottom plate that is raised 6.5" above the bottom flange. The lower disk has a 45-degree taper that fits into the center hole of the top plate and lifts the instrument into the raised position. The three positions are shown in Figure 8.

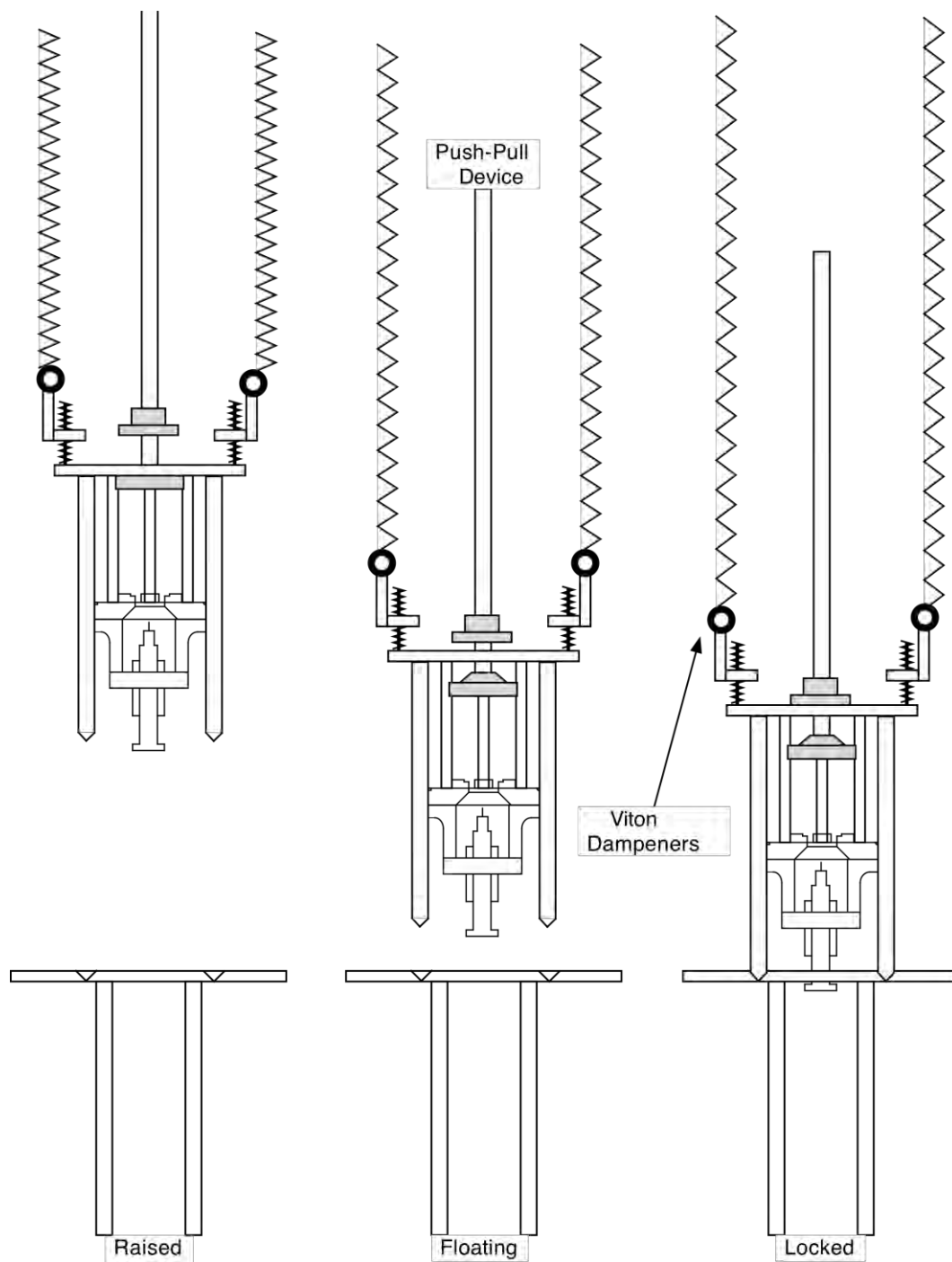


Figure 8: Three operating positions of the STM, scale 1:3

The locked position is where the STM legs are locked into the countersunk holes in the bottom plate that fit the taper on the STM legs. This position is used to change tips and to mount or dismount samples in the STM. A tip carousel and a tungsten-heating element are mounted to the bottom plate raised to the level of the sample holder. A wobble stick is used to move the tips to each station. The tips, tube scanner, and carousel all have magnetic mounts that can be gripped by the end of the wobble stick. Sample transfer is also done in this stage with the wobble stick.

The final stage is the raised position. This is used for transferring samples from different positions using a XYZ manipulator that can move samples from annealing and characterization stages into the STM position where the wobble stick can retrieve the sample and transfer into the sample holder, as shown in Figure 8.

C. Thermal isolation

Thermal expansion or contraction of the STM head assembly can affect the resolution of the instrument. The tip can drift when scanning due to small contractions and expansions in the parts that support the scanning tube and sample. [1] Materials that have low thermal expansion and conductivities are used. The UHV compatible and machinable glass-ceramic Macor was chosen because it has the desired thermal characteristics. The symmetry of the instrument is in such a way that contractions or expansions should not affect the tip to sample distance. This is because the sample holder is at the center axis and everything should contract around this point.

Macor is a silica-based material with an expansion coefficient of $\alpha_{Macor} = 9.3 \times 10^{-6} \text{ C}^{-1}$ and thermal conductivity of $K_{Macor} = 1.46 \text{ W/m}\cdot\text{K}$. The linear expansion of a material is given by

$$\Delta L = L_o \alpha \Delta T, \quad (29)$$

where ΔL is the length change, ΔT is the temperature change, and α is the expansion coefficient. [8] The temperature change that is required to change the length of a 3" piece of Macor by 1 \AA is about $1.4 \times 10^{-4} \text{ K}$. For SS304, the expansion coefficient is $\alpha_{SS} = 17.3 \times 10^{-6} \text{ m/mK}$ which results in a temperature change of $7.5 \times 10^{-5} \text{ K}$ for a 3" piece. Therefore, it is clear that Macor will have smaller expansion or contraction lengths than if the STM head was made from SS. The thermal conductivity of SS304 is $K_{SS} = 16.2 \text{ W/m}\cdot\text{K}$, which is a factor of 11 higher than Macor. This means that SS is much more sensitive to external heat sources than Macor.

The STM is designed with a thermocouple that is attached to the SS top plate to monitor the temperature during bakeout. A thermocouple works on the Seebeck effect, this is the property of metals where a temperature gradient will cause a small voltage. The thermocouple operates on this principal by using two wires that are different metals and measuring the voltage difference between them. This potential difference can then be converted to a temperature by using standard conversion tables. [12]

D. Design of Macor STM assembly

Macor has a composition listed below in the table.

Table 1: Composition of Macor [13]

Material	Approximate weight percentage
SiO ₂	46
MgO	17
Al ₂ O ₃	16
K ₂ O	10
B ₂ O ₃	7
F	4

This material can be used reliably in temperatures up to 500 °C in UHV and is a good electrical insulator. It will not outgas into a UHV environment and UHV compatible epoxy adhesives can be used. The inchworm mounts, the sample holder plate, and the electrical terminal blocks are made out of Macor. These parts are crucial for the proper operation of the instrument and are machined to very tight tolerances (0.005"). The sample holder plate includes places for three support legs that attach to the top plate as illustrated in Figure 8. These legs are 0.25" in diameter 3" in length and 120° apart. The orientation is such that these supports will not interfere with sample transfer. The sample holder plate is 3" in diameter and 0.400" thick. There is a 0.70" diameter center hole to

allow the tip to approach the sample. The hole has a 45° taper on the bottom so that the tip approach can be viewed from one of the bottom viewports of the STM chamber.

There is a .100" deep, .700" wide channel machined that will provide clearance for the sample.

There is a stainless steel U- shaped plate that is mounted centered on the slot that is machined to accept the Mo sample mount. It is held securely by BeCu springs that were hardened by heating the springs in a furnace for 3 hours. To prevent oxidation argon was injected into the furnace. This plate also has the electrical connection where the tunneling current is measured directly from the sample. Scale drawings of these parts are shown in Figure 9.

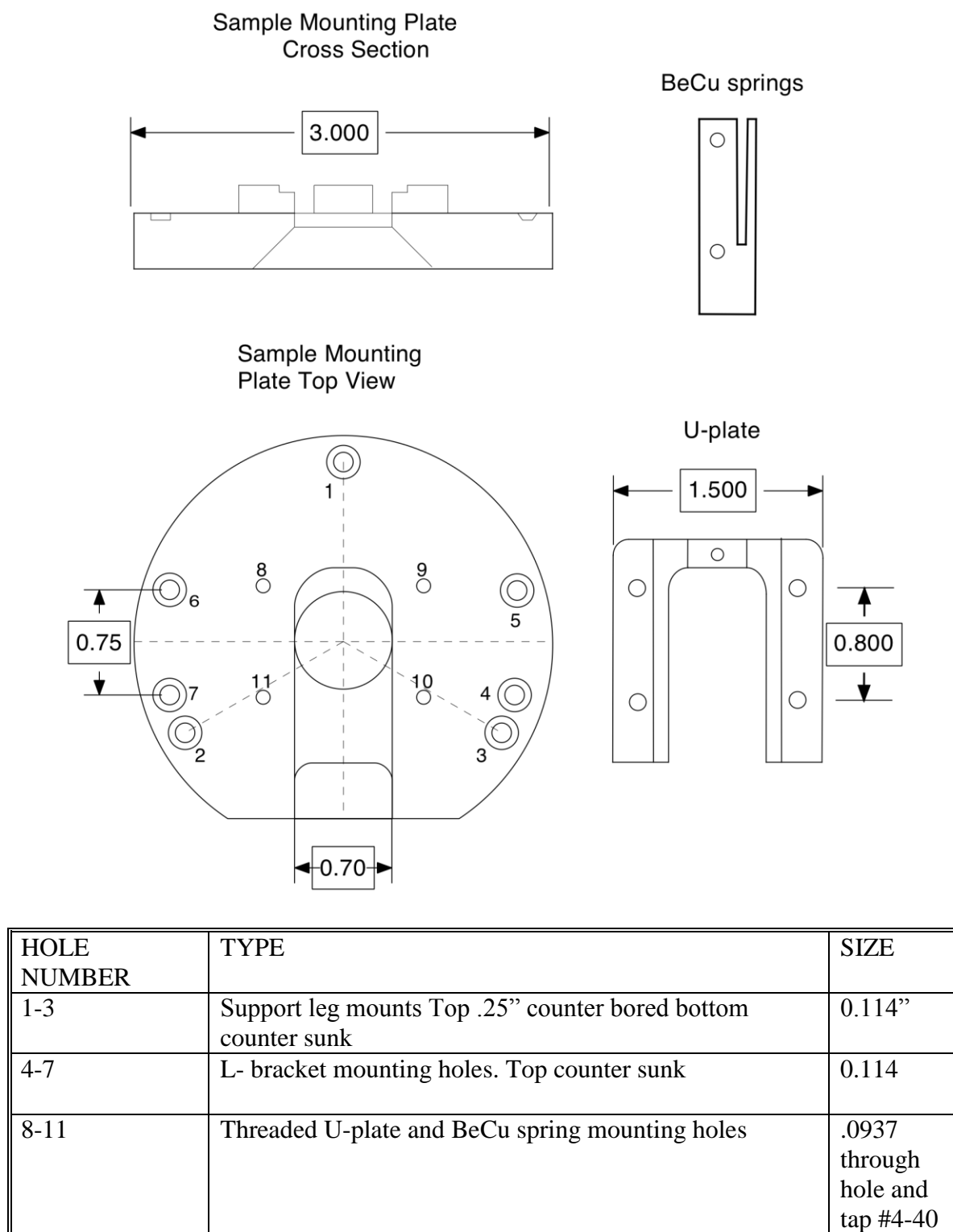


Figure 9: Sample holder assembly parts drawn 1:1 scale with a hole size table for the Macor sample mounting plate

The mount is designed for a Burleigh ARIS-11 approach module that includes the inchworm motor and tube scanner. The Module is attached to the sample holder plate by two L brackets and a mounting plate all made from Macor. A setscrew at the center plane of the mounting hole holds the module in place. These assembled parts are shown in Figure 10.

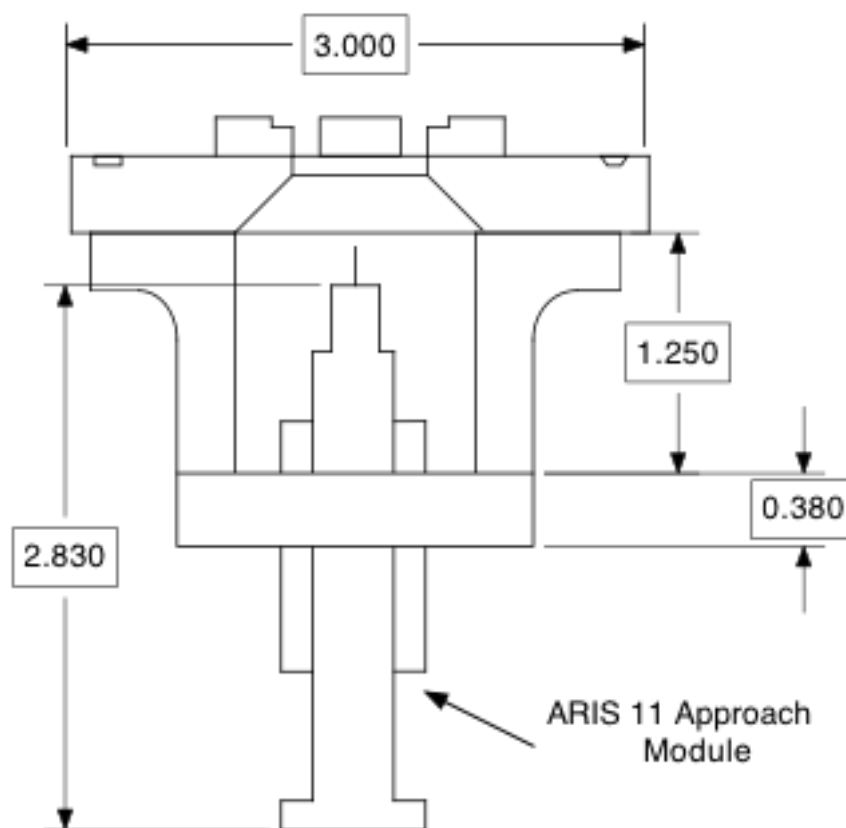


Figure 10: A 1:1 scale drawing of the STM head assembled with the Burleigh ARIS-11 approach module mounted

E. Machining Methods

To reach the tight tolerances that are needed for the STM parts, proper operation and alignment of the machining tools (*i.e.* lathes and mills) was needed. For instance, the alignment of the head of the mill and the vice for holding the machined parts was checked periodically with a dial indicator to a tolerance of 0.0005". Wear in the joints between the table and support called ways, can cause the mill table to move in a path that will not be perfectly perpendicular to the cutting plane. This will cause small variations of the z position of the piece and a stepping pattern will be cut when surfacing large areas like on the top and bottom plate. This can also cause the plate cross-section geometry to be slightly trapezoidal and not rectangular. The surfaces of the top plate need to be parallel; otherwise the support legs will not hold the STM head at the proper angle. Two mills were used for machining the STM parts: an Enco mill in the Physics shop of the Supple building and an Index mill in the Surface Science lab of the RFM building. The mill chosen to machine the top and bottom plate was the Enco mill since it had minimal wear on the ways. Parallels were used during the machining process. These are metal rectangular pieces of different thicknesses that are precision ground so that the sides are perfectly parallel to within 0.0001". The parts are mounted on the parallels inside the vice. This made it possible to smooth and flatten the surface of the plates to $\sim .002$ ".

Feed rates and cutting speeds are chosen depending on the design, material and size of the cutting bit. Typically for larger bits, slower cutting speeds and feed rates are used. The vice and parallels need to be cleaned and inspected when changing pieces, small chips can get between the sample and parallels which will misalign the sample by a

small amount. When drilling holes a shallow starting hole is drilled using a drill and countersink. This helps prevent the drill bit from drifting or chattering. The drill bit size was stepped up gradually until the proper size was reached, this is important so that the material does not heat too quickly. When drilling tapped holes, the top of the hole should be slightly countersunk. This will help the screw to mesh with the threads and lower the chance of cross threading.

A low percent thread should be used for tapped screw holes that are to be used in UHV, typically 60-65%. Whereas, most tapped holes for non-vacuum work use a percent thread of about 75%. The percent thread is a measure of how close the machined thread comes to being the same depth as the screw thread. This is determined by the diameter of the screw D , the diameter of the tap drill d , and the thread pitch P

$$\%Thread = \frac{2(D-d)}{3P \cos 30^\circ}. \quad (30)$$

This thread geometry is shown in Figure 11. [14]

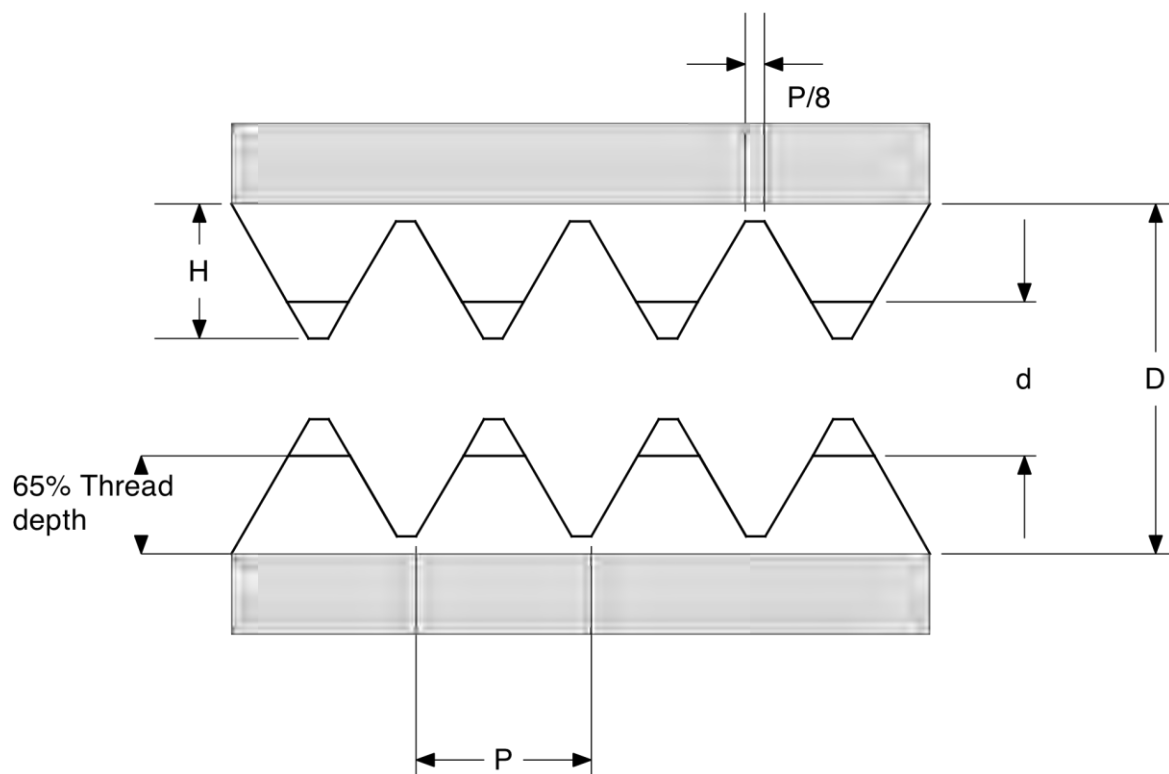


Figure 11: Geometry of standard threads

Using low thread depth percentages will help limit gas molecules from getting trapped between the threads, making it easier for any trapped gas between the threads to vent through the degas hole. For cleanliness, lubricants are not normally used under UHV; therefore, the tapped holes should have lower thread percentages to prevent seizing of the threads.

For machining SS, the end mills were made from TiCN coated high speed steel and the drill bits were made from Co steel. The TiCN coating is very hard and extends the life of the tool bit. Drill bits made from Co steel can run at much higher temperatures than those made from high speed steel. End mills with four or more flutes were used to decrease the heat generated, increase the tool life, and also to provide a better surface finish of the machined part. This is important when surfacing the top and bottom plates

since large bits are being used. A petroleum-based oil (Truedge cutting fluid) was used during the cutting process to reduce heat. The large holes on the top and bottom plate were cut to the approximate size using a bi-metal hole saw and finished with a boring head, which is a tool that can be precision adjusted for a specific hole size. This tool will give a very smooth finish for the inside surface of the hole.

The STM design uses tapped holes in the SS plates. To make a uniform and consistent thread, a Molybdenum-based lubricant is used. Using a finishing tap, a tap that has less of a taper, is important to have threads that continue to the bottom of the hole. A tap guide that mounts in the drill chuck of the mill is used to insure proper alignment between the tap and the hole. The metal chips are cleaned out after every few rotations of the tap.

The STM legs and mounting rods were machined from precision ground SS304 stock. A lathe was used to cut the rods and drill and tap the mounting holes. During the machining process a collet was used to hold the piece, and short light passes were used to avoid putting too much torque on the piece. The small diameter of these parts will increase the chance of bending. The rods need to be the same size relative to each other. The support legs and mounting rods were first cut to an approximate length on the lathe. The legs were measured and cut to within .001" of each other on the mill using a vice that has a stop that makes it possible to mount pieces in the same position each time. This is useful when duplicates of the same part like the support legs and mounting rods need to be machined. The zero position of the cutting bit will not change making it easier to machine parts that have very tight tolerances when compared to one another. For the

STM legs, a 45° taper was machined and polished, this will help the legs slide into the countersunk holes on the bottom plate.

As mentioned the entire sample holder assembly is made from Macor. This material presented machining challenges that are unique to ceramic type materials. Macor leaves an abrasive white powder when it is cut, this powder can cause wear in moving parts and readily sticks to oil. This made it important to cover the ways and any other mechanical parts near the piece that was being machined. Carbide cutting and drill bits are used to machine Macor. Macor is very abrasive, so a very hard cutting edge is needed. The surface of Macor is somewhat porous, so oil based cutting fluid is not used. The pieces need to be kept as clean as possible to avoid excess degassing inside the chamber. If Macor is heated too quickly cracking and chipping will occur to avoid this shallow cutting passes were used of approximately 0.005”.

There are several tapped holes in the Macor assembly. Specifically each L-bracket has four tapped holes and there are four tapped holed on the top of the sample holder plate. Because of the brittle nature of Macor, threads can chip and crack easily during the manufacturing process. This problem is limited by using low percent thread percentages in this case 65% or below and only rotating the tap in one direction. [13] This is different than SS where it is necessary to rotate the tap forward and backward because metal filing will get packed into the threads and cause torque on the tap, which can lead to breakage. Since Macor creates dust instead a low thread depth percentage will provide more room for the dust residue therefore reducing the torque on the tap. The screws that are used in the Macor should be installed with a low torque to avoid

damaging the brittle threads. These screws should not be removed unless necessary for the same reason.

The sample mounting plate as illustrated in Figure 8 was machined from a 3" diameter Macor cylinder. The center hole was machined first on the lathe. A cutoff tool was used to cut the piece to the desired thickness. This tool uses a thin high-speed steel blade that can make very smooth cuts. During the cutting process compressed air was used to cool the piece and the slowest feed rate possible was used. The result was a very smooth surface and the thickness matched the desired specifications. The bottom of the center hole was then tapered with a 45° angle using a boring bar. The rest of the fabrication was done on the mill using the process described above to the specifications of Figure 8. The L brackets were machined from 1 1/4" square stock using the mill. The square stock was first machined down to specifications. A side mill was then used to create an L shape by taking multiple passes in two directions. The L-shaped pieces were then separated from the square stock using a diamond edged circular saw that is cooled using a water-based lubricant so that they were slightly oversized. Using the mill, the pieces were precision machined to specifications and the mounting holes were drilled and tapped.

Following the machining process, all of the parts, including screws and washers were cleaned using an ultrasonic bath. The SS parts were first cleaned using acetone for about 40 min, followed by methanol for about 30 min. The Macor pieces were also cleaned using the ultrasonic bath, but two successive methanol cleanings were used since acetone makes the Macor porous. This cleaning process removed any dirt or oil from the manufacturing process.

F. Electronics Design

Electromagnetic interference and noise can cause a loss of resolution when operating an STM. Electromagnetic interference due to outside sources can couple to the sample current and the x , y , and z piezo drives. The UHV chamber will create a Faraday cage around the STM isolating it from interference sources outside of the chamber. Foil and braid shielded cable is used to connect the STM control electronics to the electrical feedthrus and connect the inchworm controller to the control electronics.

The inchworm is controlled by a computer signal that is sent to a Burleigh Instruments ARIS-950 inchworm controller that operates the inchworm motor as described earlier. There are four connections on the inchworm: one for the front clamp, the rear clamp, the center piezo element, and a common ground for each component. [15] The STM control electronics used were designed and constructed previously by Dr Carl Ventrice and a group of previous graduate students. Dr. Vince Labella wrote the computer software. It controls the speed and direction of the inchworm and stops the motion when a specific tunneling current is measured. It also controls the sweeping of the STM tip and acquisition of the STM images.

The STM control electronics are designed to control the tube scanner so that CCI and STS can be performed. Before the sample current can be used to drive the z motion of the tip, the current must be converted into a voltage using a current to voltage preamplifier that has a gain of either 10^8 , 10^9 , or 10^{10} V/A. After the current is converted, the signal is fed to a Logarithmic amplifier and also sent directly into the computer through an analog to digital converter (ADC) to be monitored by the STM program. The

Logarithmic amplifier has two inputs: the tunneling current I_i and a reference current input I_{ref} . [16] The output of the Log amp is

$$I_0 = \log \frac{I_i}{I_{ref}} . \quad (31)$$

Since the tunneling current is exponentially dependent on the distance between the tip apex and the surface, the Log amp converts the signal to a linear distance dependence. To perform STS a sample-and-hold amplifier is incorporated into the feedback loop. This amplifier will disable the feedback loop and hold the z -piezo at a constant voltage, which will keep the tip at a constant height while the tip bias is ramped to perform the I - V measurement. A variable gain amplifier is used before the z high voltage drive. This stage allows the proportionality constant of the feedback loop to be adjusted. If the gain is too high, the tip will tend to oscillate. If the gain is too low, the tip will not track properly. After this stage, the signal is sent to both the ADC so that the STM program can monitor the tip height and to the z high voltage driver that controls the z -axis movement of the scanning tube. The electronics also include high voltage amplifiers that control the x and y -axis movement and control the tip bias. This entire system is shown in Figure 12.

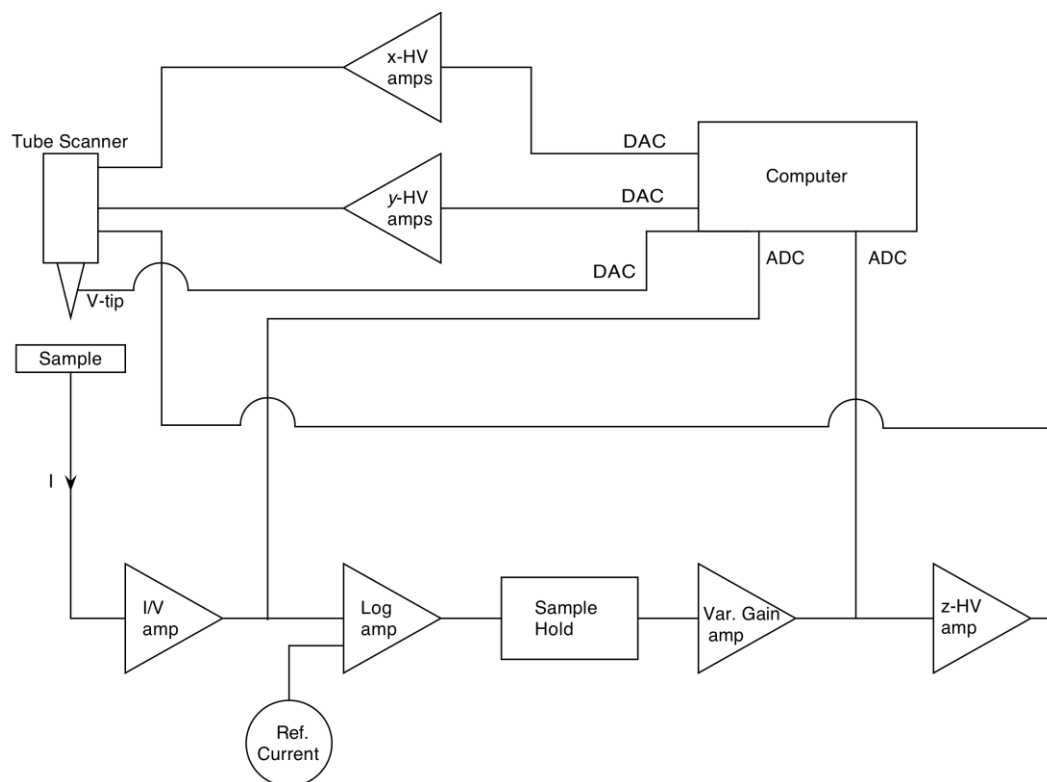


Figure 12: STM control electronics

IV. RESULTS AND DISCUSSION

As mentioned in the Introduction, the STM was designed to be incorporated into the UHV surface analysis chamber in the Surface Science Lab, as shown in Figure 13.

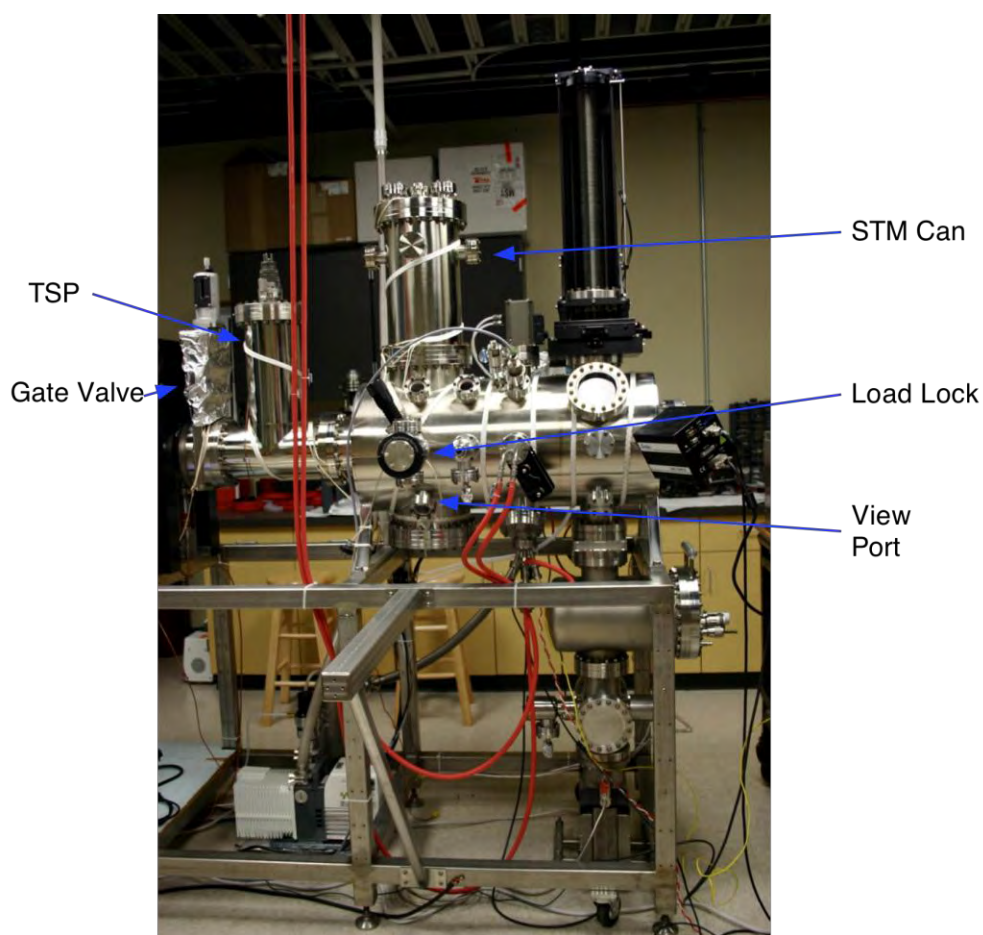


Figure 13: UHV surface analysis chamber

After the machining of all of the STM components, a thorough cleaning of each component was required so that they could be used in UHV. This was followed by the assembly of the components. The initial stage of assembly is shown in Figure 14.

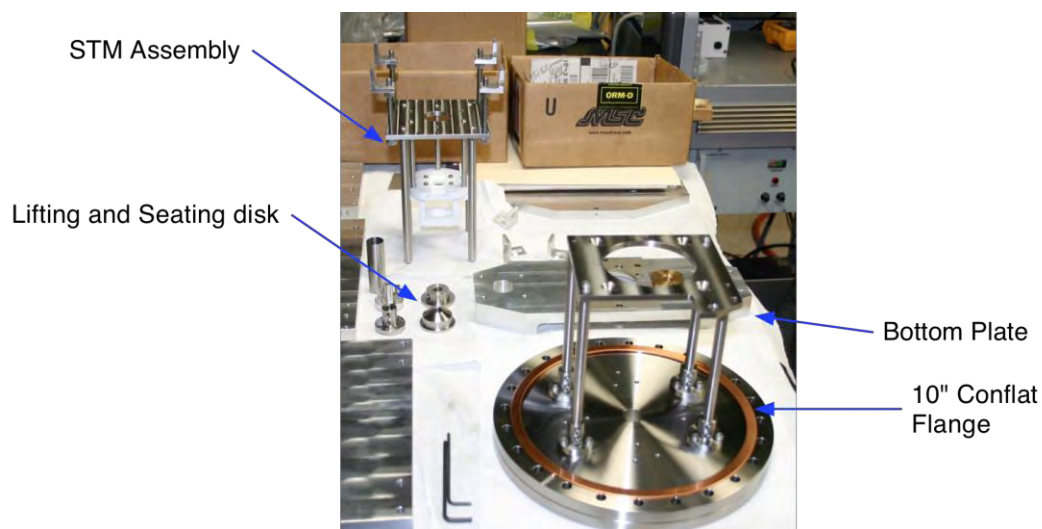


Figure 14: STM components

After complete assembly of the STM, including all wiring, it was mounted in a custom built test stand apparatus that has the same flange to flange dimension as the UHV chamber in Figure 13. The completely assembled STM in its test stand is shown in Figure 15.

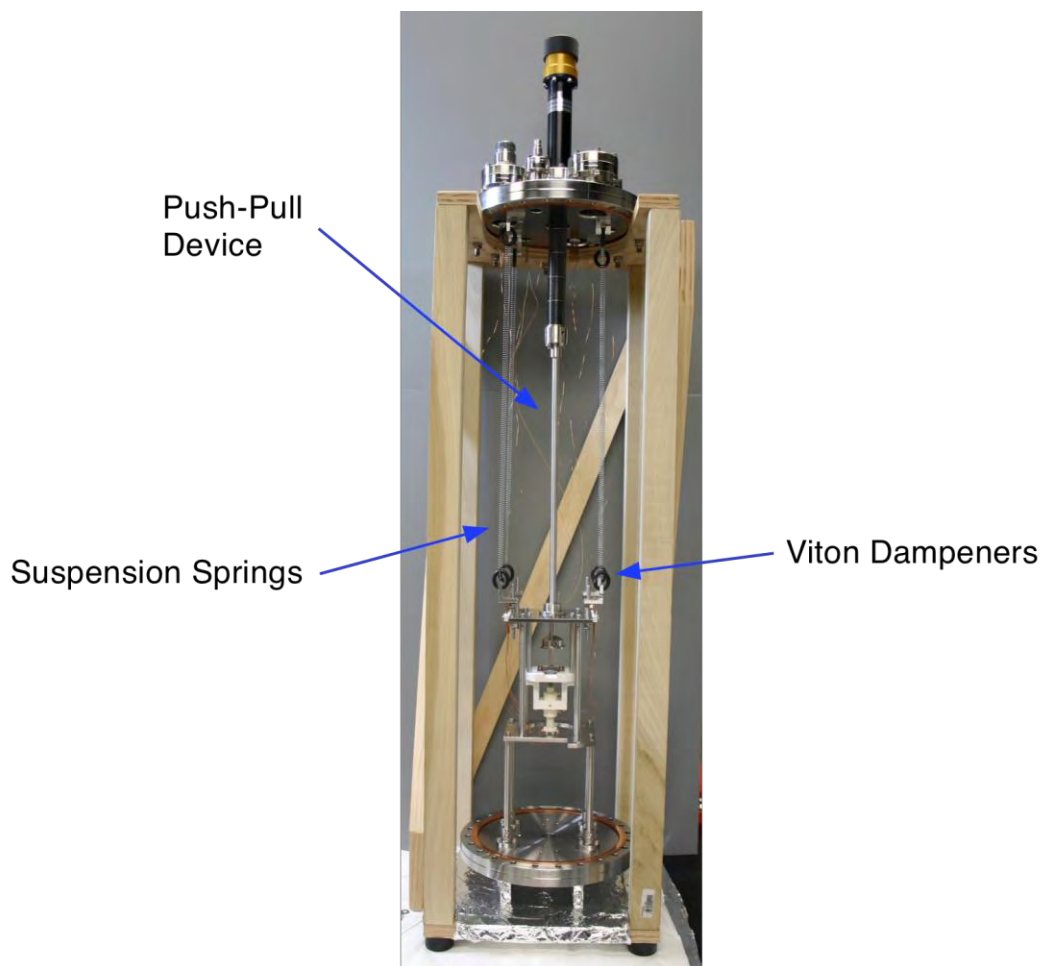


Figure 15: STM mounted on test stand

The UHV inchworm motor (ARIS 11, Approach Module) is attached to the STM head using a SS #6-32 set screw, as shown in Figure 16. The bore of the Macor mounting plate is machined only 0.002" larger in diameter than the outer diameter of the inchworm motor to provide a zero-clearance slip fit. By using a set screw, the inchworm motor height can be adjusted, or it can be removed completely if maintenance is needed. The STM tip mounts at the top of the tube scanner of the inchworm motor using a magnetic chuck. A top view of the STM head is shown in Figure 17. The sample holder

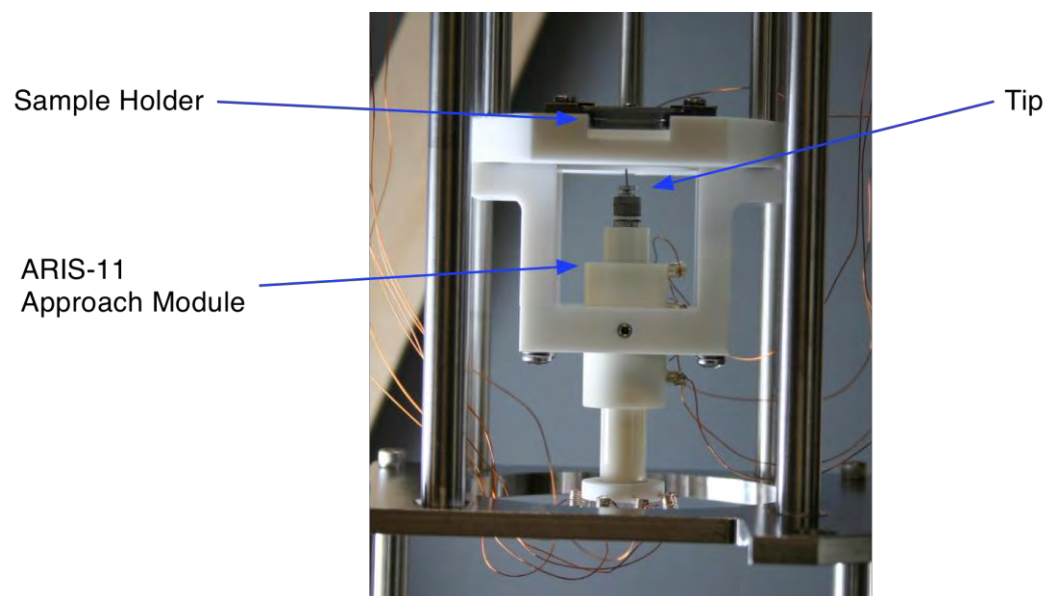


Figure 16: STM head with tip and UHV inchworm

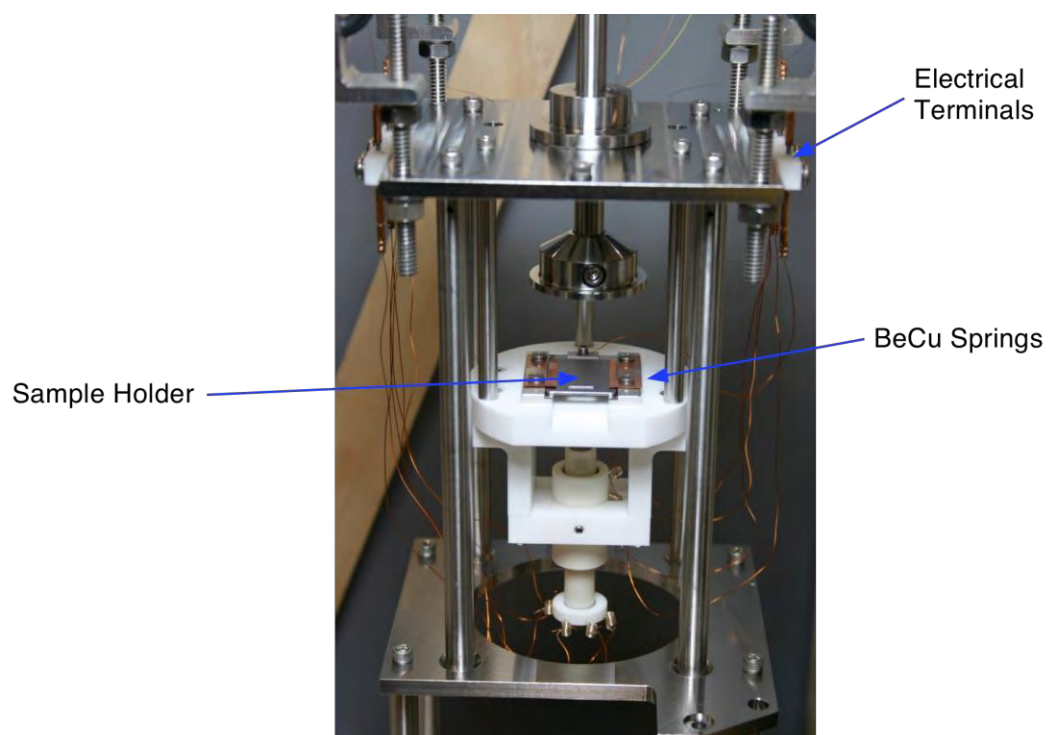


Figure 17: STM sample mount and electrical connections

plate is held in place with two hardened BeCu spring clips. The sample is attached on the bottom of the Mo sample holder plate using spot welded Ta wires. Since the SS top plate of the STM assembly is mechanically isolated from the vibrations of the top conflat flange, thicker 0.010" Capton coated wire is used to make the electrical connections to the inchworm motor and scanning tube from the Macor electrical terminal blocks.

The three operating positions of the STM are shown in Figure 18. For tip exchange and sample mounting, the STM is locked into the bottom plate. This is achieved by extending the linear motion feedthru so that the seating disk pushes the legs of the STM assembly into four countersunk holes in the bottom plate. For imaging surfaces, the STM assembly must hang only from the four stainless steel springs. This is achieved by partially retracting the linear motion feedthru so that the seating disk no longer touches the top plate of the STM. To move samples into/out of the main UHV chamber from/to the magnetic translator of the load lock or to move samples from/to the horizontal.

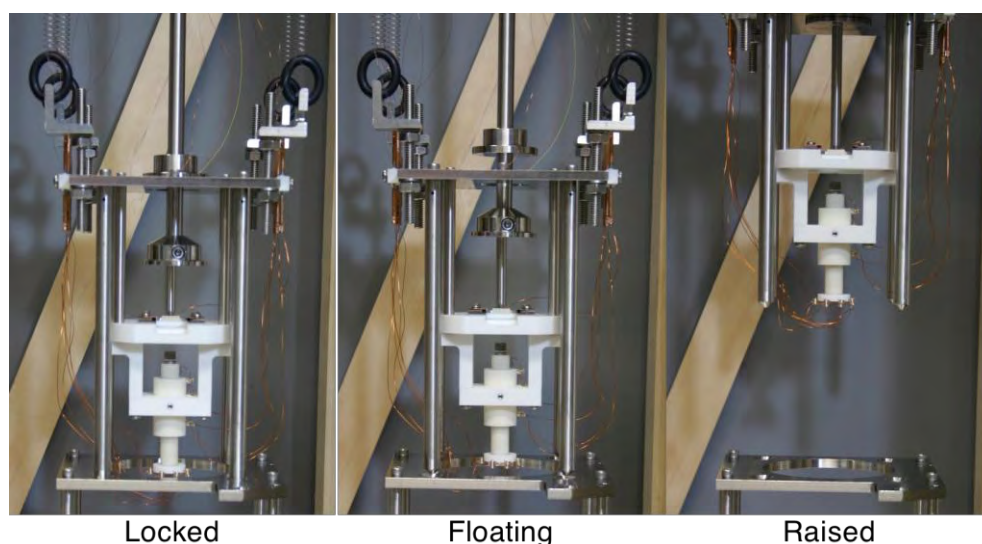


Figure 18: STM in locked, floating, and raised positions

manipulator to/from the STM head, the STM assembly must be raised above the centerline of the chamber. This is achieved by retracting the linear motion feedthru all the way so that the lifting disk engages in the top plate of the STM and lifts the STM assembly to its highest position.

At present, all of the mechanical components of the STM have been constructed and tested, which was the stated goal of this thesis project. Before the STM is used by the next graduate student for routine analysis of the atomic scale features of surfaces, further testing of the STM control electronics will need to be performed. For instance, the pickup and noise of the STM electronics needs to be tested while it is in tunneling mode inside of the UHV Surface Analysis Chamber. Since the chamber acts as a Faraday cage, the true operational conditions of the STM electronics will be achieved. It would also be convenient if the STM control and analysis software is ported to a Windows-based computer operating system. At present, the computer operating system is IBM OS2, which is no longer supported by IBM. This is an extensive project that will probably take at least a month or two to accomplish.

V. CONCLUSIONS

A STM has been constructed for the atomic-scale analysis of the surfaces of materials in UHV. All components of the STM are manufactured from UHV compatible materials. In addition, the main STM head is manufactured from Macor, which has a relatively small coefficient of expansion and a low thermal conductivity. This results in a reduction in thermal drift effects that are common in most commercial STM designs. By using a custom push-pull device, the STM can be locked in place for sample and tip transfer, floated from its springs for imaging, and raised above the centerline of the chamber to allow access to the load lock's magnetic translator or the horizontal translator of the main STM chamber. The STM uses a unique spring-mass-damper system for vibration isolation, which has a resonant frequency of less than 1 Hz. At this point, the STM is ready for further testing of the control electronics under UHV conditions before routine atomic-scale imaging of surfaces can be achieved.

REFERENCES

- [1] Ventrice, C. A., Labella, V., & Schowalter, L. J., *Design of a scanning tunneling microscope for in-situ topographic and spectroscopic measurements within a commercial molecular beam epitaxy machine*, J. Vac. Sci. Technol. A **15**, 830-835 (1997).

- [2] Serway, R. A., Moses, C. J., & Moyer, C. A., *Modern Physics* (Thomson Brooks/Cole, Belmont, 2004) Ch. 4.

- [3] Liboff, R. L., *Introductory Quantum Mechanics* (Addison Wesley, Boston, 2003) 4th Edition, Ch. 7, p. 219.

- [4] Wiesendanger, R., *Scanning Probe Microscopy and Spectroscopy Methods and Applications* (Cambridge University Press, Cambridge, 1994).

- [5] Singh, J., *Quantum Mechanics: Fundamentals and Applications to Technology* (John Wiley and Sons, New York, 1997).

- [6] *ARIS-950/ULN Inchworm Controller Operating Manual* (Burleigh Instruments, Fishers, 1994).

- [7] DiNardo, N. J., *Nanoscale Characterization of Surfaces and Interfaces* (VCH, New York, 1994).

- [8] Halliday, D., Resnick, R., & Walker, J., *Fundamentals of Physics* (John Wiley and Sons Inc, Hoboken, 2005).

- [9] Ohring, M., *Material Science of Thin Films* (Academic Press, New York,) 2nd Edition.

- [10] *Atlas Steels-Specialty Steels Product Reference Manual* (Atlas Steel, Australia, 2000).

- [11] Thornton, S. T., & Marion, J. B., *Classical Dynamics of Particles and Systems* (Thomson Brooks/Cole, New York, 2004) 5th Edition.
- [12] *Omega Temperature Measurement Handbook & Encyclopedia* (Omega Engineering, Stamford, 1992)
- [13] *Macor Lighting and Materials Reference Manual* (Corning Inc., Corning, 2001).
- [14] Shigley, E. S., & Mitchell, L. D., *Mechanical Engineering Design* (McGraw-Hill, New York, 1983).
- [15] *ARIS-10/11 Approach Module Operating Manual* (Burleigh Instruments, Fishers, 1994).
- [16] *LOG100: Precision Logarithmic and Log Ratio Amplifier Reference Manual* (Burr-Brown, Dallas, 1995).

VITA

Robert Steven Kilbourn was born November 3, 1983 in Houston Texas to Mary and Robert Glen Kilbourn. He has two older brothers David and Michel Kilbourn and two younger half sisters Renee and Rebecca Kilbourn. Robert attended middle and the first year of high school in Naperville IL. In 1999 he moved with his Father and Stepmother to Austin Texas where he graduated from James Bowie high school in 2002.

Robert then started attending Texas State University-San Marcos in the fall of 2002. While attending college he worked part time as a full service auto mechanic and a teachers assistant in the physics department. He started undergraduate research for Dr. Carl Ventrice in the fall of 2007. After five years of undergraduate studies he was awarded a Bachelor's of science degree in physics in December of 2007.

In the Spring of 2008 Robert began graduate school at Texas State University-San Marcos. He began graduate research in STM design and completed the construction of the mechanical components of a UHV room temperature STM.

Permanent Address: 4000 Quail Run
San Marcos TX 78666

This thesis was typed by Robert S. Kilbourn.